MOLECULAR AND CELLULAR BIOLOGY, Oct. 2011, p. 3997–4006 Vol. 31, No. 19
0270-7306/11/$12.00 doi:10.1128/MCB.05808-11

Pirh2 E3 Ubiquitin Ligase Monoubiquitinates DNA Polymerase Eta To Suppress Translesion DNA Synthesis▽†

Yong-Sam Jung,[1] Anne Hakem,[2,3] Razqallah Hakem,[2,3] and Xinbin Chen[1]*

Comparative Oncology Laboratory, University of California, Davis, California 95616,[1] and Department of Medical Biophysics, University of Toronto,[2] and Ontario Cancer Institute, University Health Network,[3] Toronto, Ontario, Canada

Received 14 June 2011/Returned for modification 28 June 2011/Accepted 18 July 2011

Polymerase eta (PolH) is necessary for translesion DNA synthesis, and PolH deficiency predisposes xeroderma pigmentosum variant (XPV) patients to cancer. Due to the critical role of PolH in translesion DNA synthesis, the activity of PolH is tightly controlled and subjected to multiple regulations, especially posttranslational modifications. Here, we show that PolH-dependent lesion bypass and intracellular translocation are regulated by Pirh2 E3 ubiquitin ligase through monoubiquitination. Specifically, we show that Pirh2, a target of the p53 tumor suppressor, monoubiquitinates PolH at one of multiple lysine residues. We also show that monoubiquitination of PolH inhibits the ability of PolH to interact with PCNA and to bypass UV-induced lesions, leading to decreased viability of UV-damaged cells. Moreover, we show that monoubiquitination of PolH alters the ability of PolH to translocate to replication foci for translesion DNA synthesis of UV-induced DNA lesions. Considering that Pirh2 is known to be overexpressed in various cancers, we postulate that in addition to mutation of PolH in XPV patients, inactivation of PolH by Pirh2 via monoubiquitination is one of the mechanisms by which PolH function is controlled, which might be responsible for the development and progression of some spontaneous tumors wherein PolH is not found to be mutated.

The hereditary material of an organism is under constant attack by endogenous genotoxic stresses and exogenous sources such as UV light and alkylation agents. UV light causes DNA lesions that block the accurate and processive DNA synthesis. Although the majority of DNA damage is recovered by excision repair systems, the remaining DNA lesions can hinder the activity of DNA polymerase during S phase (11). Under these conditions, many organisms require the action of specialized translesion DNA polymerases that can bypass various DNA lesions (6, 8, 27). Many of these translesion DNA synthesis (TLS) polymerases, including PolH, belong to the Y-family DNA polymerases (8, 27). Xeroderma pigmentosum variant (XPV) cells were unable to replicate past UV-induced DNA lesions due to inactivating mutations in the PolH gene (14, 24). Thus, it is postulated that PolH-mediated replication bypass across these DNA lesions is particularly important to prevent UV-induced carcinogenesis in XPV patients.

Ubiquitin (Ub) was originally identified as a 76-amino-acid (aa) ubiquitous, eukaryotic protein. Ubiquitin is conjugated to target proteins via an isopeptide bond between the C terminus of ubiquitin and a lysine residue; thereby, ubiquitinated proteins can be degraded by the 20S proteasome (13). In addition, ubiquitin can serve as a reversible modification that regulates the activity of target proteins without proteasomal degradation, such as signal transduction, autophagy, chromatin remodeling, membrane trafficking, and DNA repair (9). The conjugation of a single ubiquitin molecule to a target protein is known as monoubiquitination. Histones, membrane proteins, and ubiquitin binding domain (UBD)-containing proteins are usually monoubiquitinated (1, 9, 12, 25). Due to the requirement of a functional UBD, monoubiquitination of UBD-containing proteins is referred to as coupled monoubiquitination, which is also used as a signal for proteasomal degradation (3, 4, 18).

Previously, we showed that Pirh2 physically interacts with PolH and subsequently promotes PolH degradation (16). However, Pirh2 does not catalyze PolH polyubiquitination. In addition, recent studies showed that the ubiquitination status of PolH controls its interaction with PCNA (1, 2, 26). These findings prompted us to examine whether Pirh2 monoubiquitinates PolH and regulates PolH-mediated TLS. Here, we demonstrated that Pirh2 promotes PolH monoubiquitination at K682, K686, and K694, located within the nuclear localization signal (NLS), and at K709. We also found that that Pirh2-mediated monoubiquitination inhibits PolH to interact with PCNA and its ability in the translesion DNA synthesis of UV-induced DNA lesions, which leads to decreased viability of UV-damaged cells. Our results indicate that Pirh2-mediated monoubiquitination is a mechanism by which PolH expression and activity are controlled.

MATERIALS AND METHODS

Cell culture. RKO, Pirh2-KD RKO (clone 11) in which Pirh2 can be inducibly knocked down, and primary human fibroblasts derived from XPV patients (GM03617) were used as described previously (21). Wild-type and Pirh2-knockout mouse embryonic fibroblast (MEF) cells were generated from 13.5-day embryos according to standard procedures.

Generation of Pirh2-knockout mice and Pirh2-knockout MEFs. Embryonic stem (ES) cells were electroporated with a linearized target construct to generate $Pirh2^{fl2\text{-}3\text{-}neo}$ ES clones. $Pirh2^{\Delta 2-3}$ ES clones lacking exons 2 and 3 and a neomycin resistance cassette were obtained following transient transfection of two targeted $Pirh2^{fl2\text{-}3\text{-}neo}$ ES clones with cytomegalovirus (CMV)-Cre recombinase. All mice were in 129/C57BL/6 genetic background and were maintained in the animal facility of the Ontario Cancer Institute in accordance with the established

* Corresponding author. Mailing address: Comparative Oncology Laboratory, University of California, Davis, CA 95616. Phone: (530) 754-8404. Fax: (530) 752-6042. E-mail: xbchen@ucdavis.edu.

† Supplemental material for this article may be found at http://mcb.asm.org/.

▽ Published ahead of print on 26 July 2011.

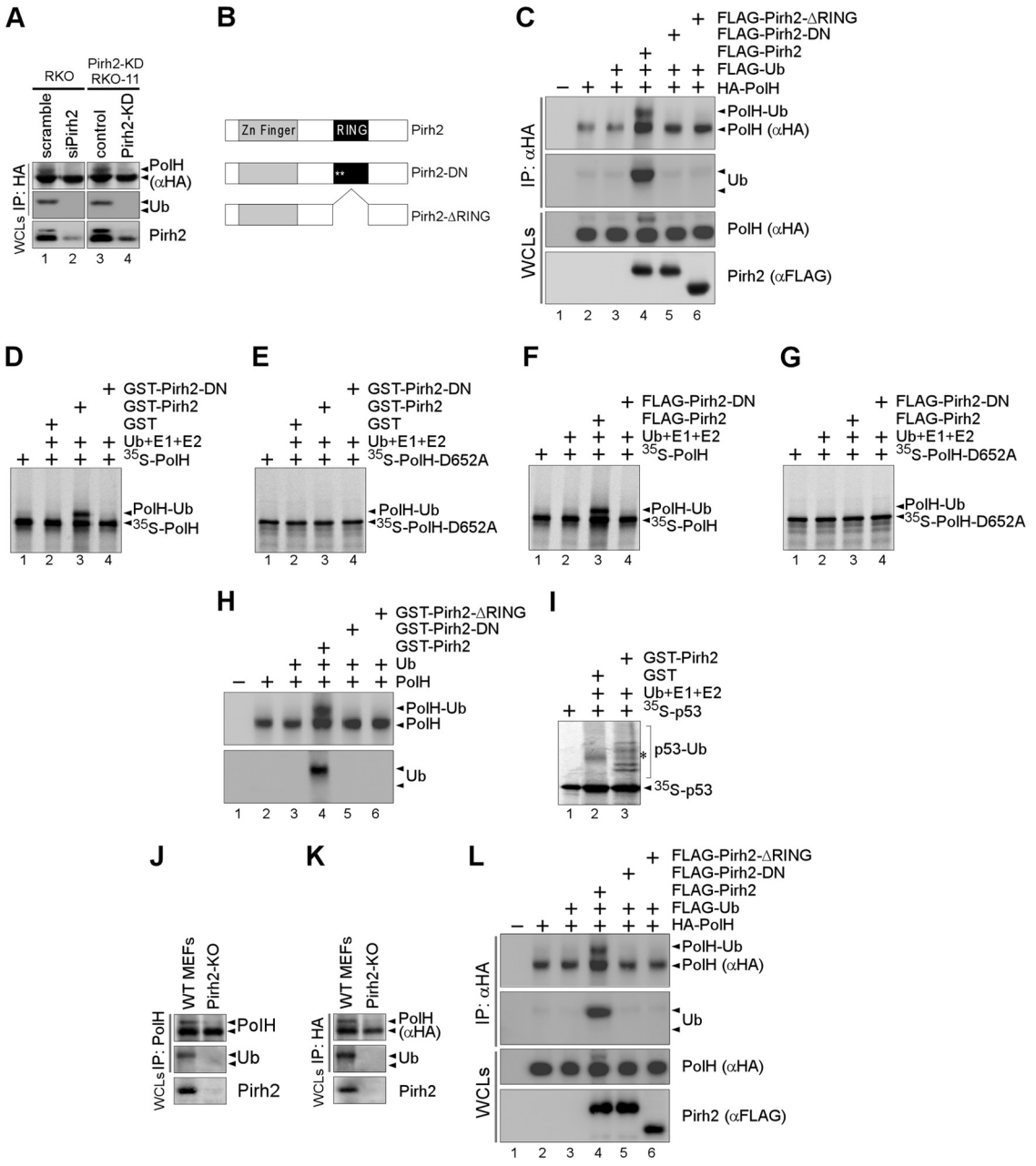

FIG. 1. Pirh2 promotes PolH monoubiquitination. (A) Whole cell lysates (WCLs) were prepared from RKO cells transfected with HA-PolH along with Pirh2 siRNA or uninduced or induced to express Pirh2 shRNA for 72 h. The lysates were then used for Western blotting with anti-Pirh2 (bottom panel) as well as subjected to immunoprecipitation with anti-HA followed by Western blotting with anti-HA to detect PolH and antiubiquitin (top panels). (B) Schematic presentation of Pirh2 domains (RING, RING finger E3 ubiquitin ligase domain; Zn Finger, CHY zinc finger domain), along with locations of mutations and deletions. (C) Cell lysates were prepared 6 h following MG132 (5 μM) treatment from RKO cells transfected with HA-PolH along with ubiquitin and wild-type or mutant Pirh2. The lysates were then used for Western blotting with anti-FLAG (αFLAG) to detect Pirh2 or anti-HA (αHA) to detect PolH (bottom panel) as well as subjected to immunoprecipitation with anti-HA followed by Western blotting with anti-HA to detect PolH and antiubiquitin (top panels). (D to E) *In vitro* ubiquitination of PolH and PolH-D652A was performed with recombinant GST-Pirh2 and Pirh2-DN along with E1, E2, and ubiquitin. ^{35}S-labeled PolH and PolH-D652A were separated on SDS-PAGE gel and analyzed by autoradiography. (F and G) The experiments were carried out as in panels D and E, except that immunopurified Pirh2 and Pirh2-DN were used as an E3 ubiquitin ligase. (H) The experiments were carried out as in panels D and E, except that recombinant PolH protein was used as a substrate. PolH and PolH-Ub were detected by anti-PolH (top panel), whereas ubiquitin was detected by antiubiquitin (bottom panel). (I) The experiment was carried as in panels D and E, except that ^{35}S-labeled p53 was used as a substrate. An asterisk indicates a nonspecific band. (J) Cell lysates were purified from wild-type and Pirh2-KO MEF cells and then used for Western blotting with anti-Pirh2 (bottom panel) as well as subject to immunoprecipitation with anti-Pirh2, followed by Western blotting with anti-Pirh2 and antiubiquitin (top panels). (K) The experiment was performed as in panel J, except that MEF cells were transfected with HA-PolH and anti-HA was used for immunoprecipitation and Western blot analysis. (L) The experiment was performed as in panel C, except that Pirh2-KO MEF cells were used.

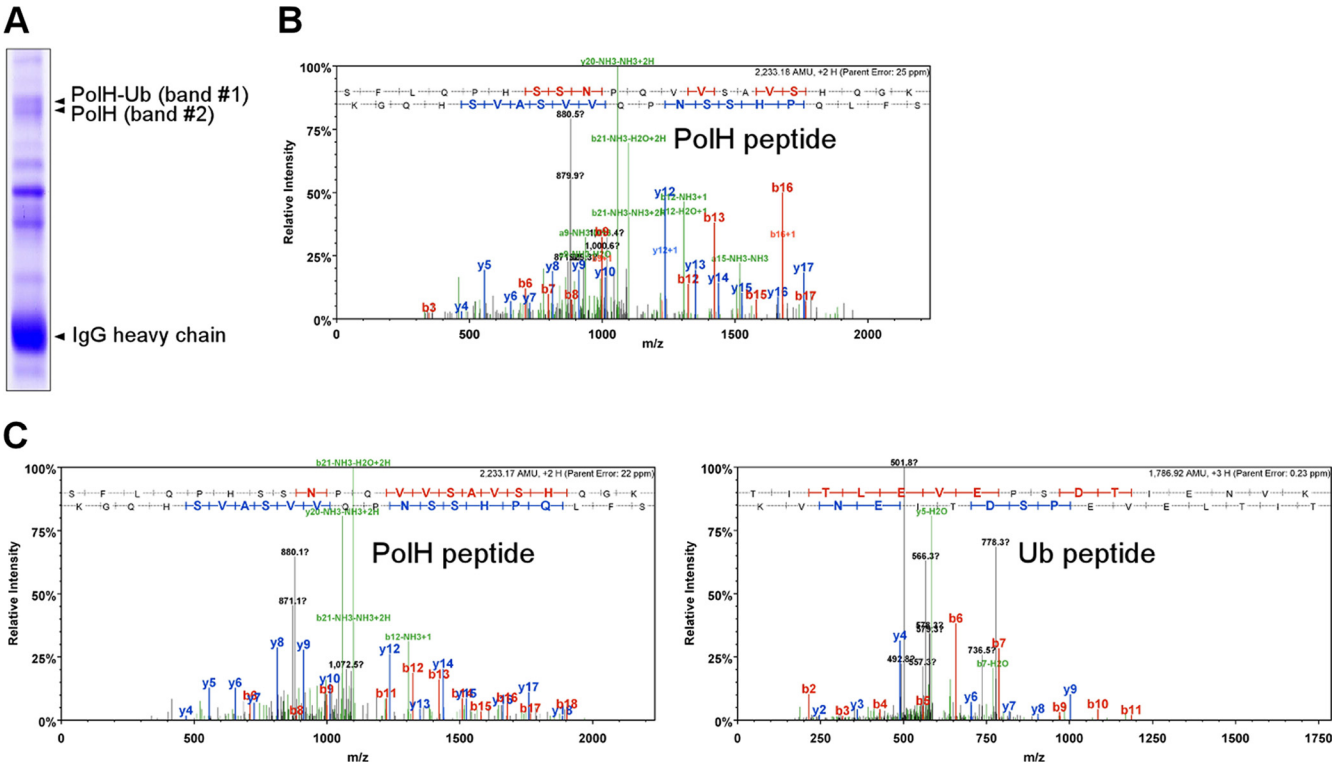

FIG. 2. Characterization of PolH and monoubiquitinated PolH. (A) RKO cells were cotransfected with HA-tagged PolH and FLAG-tagged Pirh2. After immunoprecipitation of RKO cell extracts with anti-HA antibody, the immunocomplex was separated and visualized by Coomassie blue stain. The bands corresponding to PolH (band 2) and monoubiquitinated PolH (band 1) were cut out and then subjected to mass spectrometry. (B) Band 2 was subjected to in-gel tryptic digestion and analyzed by mass spectrometry using an LTG-FT Ultra ion trap mass spectrometer as described in Materials and Methods. A representative peptide sequence of PolH from band 2 is shown at the top of the mass spectrum. (C) Band 1 was analyzed as described in panel B. Representative peptide sequences of PolH and ubiquitin from band 1 are shown at the top of the mass spectra.

ethical care regulations of the Canadian Council on Animal Care. The 13.5-day embryos were used to generate MEF cells according to standard procedures.

Antibodies. Anti-PCNA, rabbit polyclonal and mouse monoclonal anti-PolH, mouse antiubiquitin, and rabbit anti-Pirh2 were purchased from Santa Cruz Biotechnology. The other antibodies were antihemagglutinin (anti-HA) (HA11; Covance), anti-FLAG (Sigma), anti-p53 (DO-1, PAb1801, PAb240, and PAb421), and antiactin (Sigma).

Immunoprecipitation-Western blot analyses. The immunoprecipitation-Western blotting experiment was carried out as described previously (16). Three hundred to 500 μg of total proteins was immunoprecipitated with 2 μg of various antibodies and then subjected to Western blot analysis.

siRNA. Scramble and Pirh2 small interfering RNAs (siRNAs) (sense 5′-CCA ACA GAC UUG UGA AGA A dTdT-3′ and antisense 5′-UUC UUC ACA AGU CUG UUG G dTdT-3′) were purchased from Dharmacon.

Plasmids and mutagenesis. pcDNA3 vectors expressing HA-PolH, FLAG-PolH, FLAG-PolH-D652A, FLAG-ubiquitin, Pirh2, FLAG-Pirh2, FLAG-Pirh2-DN, and FLAG-Pirh2-ΔRING were described previously (16). FLAG-PolH-Ub was constructed by in-frame insertion of ubiquitin at the end of the PolH coding sequence.

Replacement of lysine(s) with arginine(s) in PolH was generated by site-directed mutagenesis (Quick Change; Stratagene). The following primers were used: forward primer K682R-FR (5′-GTA TCT CAT CAA GGC AGA AGA AAT CCC AAG AGC-3′) and reverse primer K682R-RR (5′-GCT CTT GGG ATT TCT TCT GCC TTG ATG AGA TAC-3′) for PolH-K682R, forward primer K694R-FR (5′-TTG GCC TGC ACT AAT AGA CGC CCC AGG CCT GAG-3′) and reverse primer K694R-RR (5′-CTC AGG CCT GGG GCG TCT ATT AGT GCA GGC CAA-3′) for PolH-K694R, forward primer K709R-FR (5′-CAA CTG GAT CCG AGA TGG ATT TGG CCC ACA ACA GCC AAA G-3′) and reverse primer K709R-RR (5′-CTA ATG TGT TAA TGG CCT AAA AAA TGA TTC CAA-3′) for PolH-K709R, and forward primer K682.686R-FR (5′-GGC AGA AGA AAT CCC AGG AGC CCT TTG GCC TGC-3′) and reverse primer K682.686R-RR (5′-GCA GGC CAA AGG GCT CCT GGG ATT TCT TCT GCC-3′) for PolH-K682.686R. Other constructs (PolH-K682.694R, PolH-K682.709R, PolH-K682.686.709R, PolH-K682.694.709R, PolH-K682.686.694R, and PolH-K682.686.694.709R [PolH-4KR]) were generated by combining single or double K-R mutations. PolH-4KR-NLS construct was generated by in-frame insertion of 2× NLS sequence from the SV40 large T antigen at the end of the PolH-4KR coding sequence. Green fluorescent protein (GFP)-tagged PolH, PolH-4KR, PolH-4KR-NLS, and PolH-Ub were cloned in pEGFP-C1 for imaging.

GST pulldown assay. Glutathione *S*-transferase (GST)-tagged Pirh2, Pirh2-DN, and PCNA were expressed by pGEX-4T-3 (Amersham Pharmacia Biotech). The GST pulldown assay was performed as described previously (15).

Ubiquitination assay. The ubiquitination assay was performed as described previously (20) with *in vitro*-synthesized ^{35}S-labeled PolH, PolH-D652A, p53 (the TNT T7-coupled reticulocyte lysate system; Promega), or recombinant PolH along with E1, E2, and ubiquitin (Boston Biochem). ^{35}S-labeled proteins were separated on an SDS-PAGE gel and analyzed by autoradiography.

Immunofluorescence assay. FLAG-PCNA along with GFP-tagged wild-type or mutated PolH was cotransfected into XPV cells on coverslips in 6-well plates. Six hours after UV irradiation (15 J/m^2), cells were fixed with formaldehyde and then incubated with primary antibody followed by secondary antibody. Nuclei were visualized using 4′,6-diamidino-2-phenylindole (DAPI).

DNA histogram analysis. DNA histogram analysis was performed as previously described (21). Both floating cells in the medium and live cells on the plates were collected 24 h following 15 J/m^2 UV irradiation.

Mass spectrometric analysis. The samples were run in one-dimensional SDS-PAGE, and potential PolH-containing bands were cut out, which were then subjected to in-gel tryptic digestion overnight. The Paradigm MG4 high-performance liquid chromatography (HPLC) system (Michrom Bioresources, Auburn, CA), which is coupled to a Thermo Finnigan LTQ-FT Ultra ion trap mass spectrometer (Thermo Fisher) through a Michrom advance captive spray ion-

ization source, was used for peptide separation and analysis. Each sample was loaded onto a trap column (Zorbax300SB C_{18}, 5 μm, 5 by 0.3 mm; Agilent Technologies, Santa Clara, CA) and desalted online. Peptides were then eluted from the trap and separated by a reverse-phase Michrom Magic C_{18} AQ (200-μm by 150-mm) capillary column at a flow rate of 2 μl/min. Samples were resuspended in 2% acetonitrile (ACN) and 0.1% trifluoroacetic acid (TFA) as the running buffer and directly loaded onto the mass spectrometer. The mass spectrometer was operated with a spray voltage of 1.2 kV, a heated capillary temperature of 200°C, and a full scan range with a mass/charge ratio of 300 to 1,400. The protein database (both canonical and isoform versions) was downloaded from Uniprot.org. The cRAP (Common Repository of Adventitious Proteins) Database, which contains the most common contaminants of samples, such as human keratin, bovine serum albumin, etc., was appended to the database to identify contaminations prior to analysis.

Clonogenic assay. XPV (GM03617) cells on 100-mm and 60-mm culture dishes in triplicate were transfected with a control vector or a vector expressing PolH, PolH-Ub, PolH-4KR, or PolH-4KR-NLS for 24 h. Cells were then washed with phosphate-buffered saline (PBS) and exposed to UV irradiation (0 to 9 J/m^2). After UV irradiation, cells were incubated in minimal essential medium (MEM) containing 0.375 mM caffeine for 13 days (2). Caffeine sensitizes XPV cells but not normal human fibroblast cells (such as GM00024 cells) upon UV irradiation. Colonies were stained with Giemsa staining solution and counted.

RESULTS

Pirh2 promotes PolH monoubiquitination. Recently, we showed that Pirh2 physically interacts with PolH and promotes PolH degradation via 20S proteasome, but Pirh2 does not polyubiquitinate PolH (16). In addition, other studies showed that the status of PolH monoubiquitination controls its interaction with PCNA (1, 2, 26). These findings prompted us to examine whether Pirh2 monoubiquitinates PolH and regulates its translesion DNA synthesis (TLS) activity. To test this, PolH ubiquitination was examined in RKO cells in which endogenous Pirh2 was knocked down by Pirh2 siRNA or inducibly knocked down by Pirh2 short hairpin RNA (shRNA) along with ectopic expression of HA-tagged PolH. We showed that the level of Pirh2 was significantly decreased by Pirh2 siRNA or shRNA (Fig. 1A, Pirh2 panel, compare lanes 1 and 3 with 2 and 4, respectively). Next, HA-tagged PolH expressed in RKO cells was immunoprecipitated by anti-HA and then used for Western blot analysis. We found that HA-PolH was detected along with a slow-migrating band recognized by anti-HA antibody (Fig. 1A, lanes 1 and 3). In addition, the slow-migrating band was markedly decreased upon knockdown of Pirh2 (Fig. 1A, compare lanes 1 and 3 with 2 and 4, respectively). Interestingly, we found that the slow-migrating band was recognized by antiubiquitin antibody (Fig. 1A, Ub panel). Based on the migration pattern, it is likely that the slow-migrating band is a monoubiquitinated form of PolH.

To validate PolH monoubiquitination, RKO cells were cotransfected with HA-tagged PolH, FLAG-tagged ubiquitin along with wild-type Pirh2, E3 ligase-deficient Pirh2-DN, or Pirh2-ΔRING (Fig. 1B). Pirh2-DN contains amino acid substitutions (C145S and C148S) in the RING finger domain, whereas Pirh2-ΔRING lacks the entire RING finger domain from aa 145 to 186 (16, 20, 23, 28). Upon immunoprecipitation with anti-HA antibody followed by Western blot analysis, we showed that a slow-migrating band was detected in cells cotransfected with wild-type Pirh2, but not Pirh2-DN and Pirh2-ΔRING (Fig. 1C, compare lane 4 with lanes 5 and 6). In addition, the slow-migrating band was found to be recognized by antiubiquitin (Fig. 1C, Ub panel, lane 4).

To investigate whether PolH is a substrate of Pirh2 E3 ligase, ubiquitination assay was performed with *in vitro*-translated ^{35}S-labeled PolH (PolH) or PolH-D652A. PolH-D652A, which contains a substitution (D652A) in the UBZ domain, is unable to interact with ubiquitin (1). We showed that PolH was monoubiquitinated in the presence of recombinant GST-tagged Pirh2 (Fig. 1D, lane 3) or Flag-tagged Pirh2 purified from RKO cells (Fig. 1F, lane 3). In contrast, Pirh2-DN was inert (Fig. 1D and F, lane 4). In addition, Pirh2 and Pirh2-DN were incapable of monoubiquitinating PolH-D652A (Fig. 1E and G). To further investigate whether PolH is a direct substrate of Pirh2, the *in vitro* ubiquitination assay was performed with recombinant PolH and showed that PolH was found to be monoubiquitinated by Pirh2, but not Pirh2-DN and Pirh2-ΔRING (Fig. 1H). As a control, p53 was polyubiquitinated by recombinant GST-tagged Pirh2 but not by GST tag alone (Fig. 1I).

To validate the role of Pirh2 in PolH monoubiquitination, we examined the status of PolH monoubiquitination in Pirh2 knockout mouse embryo fibroblast (MEF) cells. We found that endogenous PolH was monoubiquitinated in Pirh2-competent but not Pirh2-deficient MEF cells (Fig. 1J). We also found that ectopically expressed PolH was monoubiquitinated in Pirh2-competent but not Pirh2-deficient MEF cells (Fig. 1K). In addition, we showed that ectopically expressed PolH was

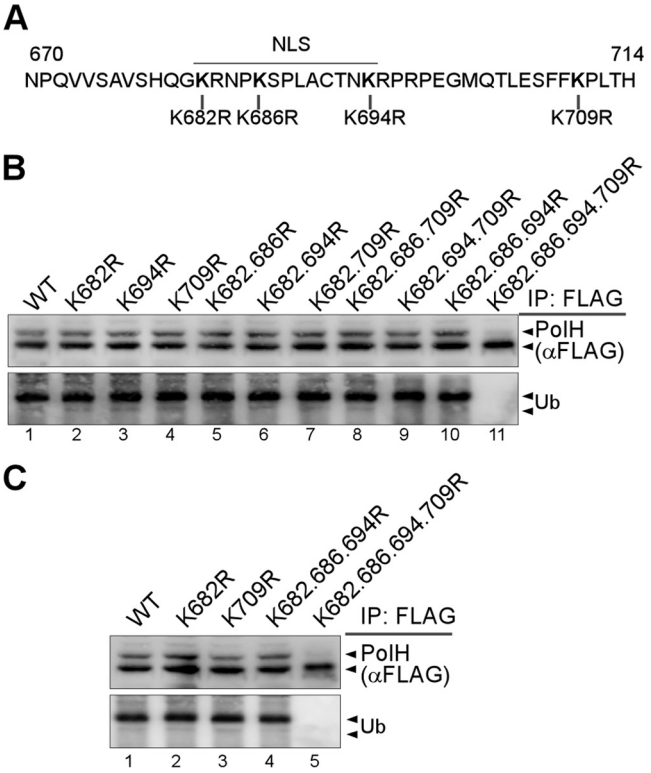

FIG. 3. Identification of lysine residues in PolH for monoubiquitination by Pirh2. (A) Locations of the nuclear localization signal and lysine-to-arginine substitution(s). (B and C) Cell lysates were prepared from RKO cells (B) or Pirh2-KO MEF cells (C), which were transfected with FLAG-tagged wild-type (WT) or mutated PolH along with HA-tagged ubiquitin and Pirh2. The lysates were then immunoprecipitated with anti-FLAG followed by Western blotting with anti-FLAG to detect PolH and antiubiquitin.

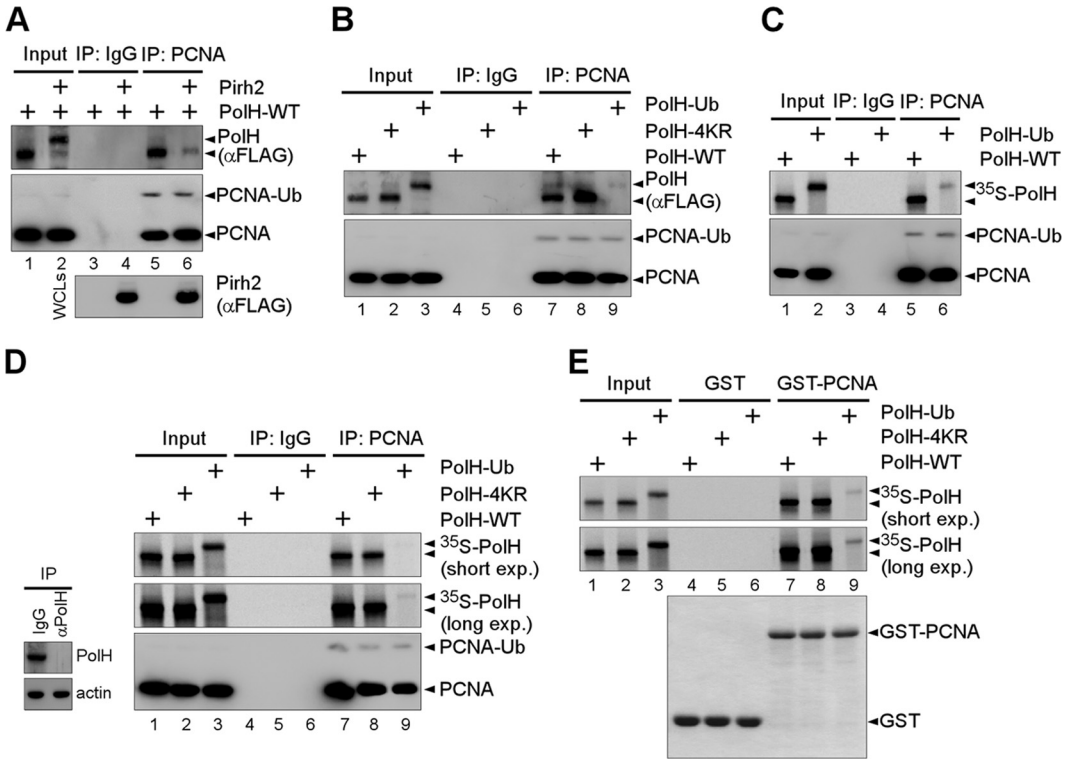

FIG. 4. Monoubiquitination of PolH disrupts its interaction with PCNA. (A) Cell lysates were prepared from RKO cells transfected with FLAG-tagged PolH and Pirh2. The lysates were then used for Western blotting with anti-FLAG (αFLAG) to detect Pirh2 (bottom panel) as well as subjected to immunoprecipitation with anti-PCNA or control IgG followed by Western blotting with anti-FLAG to detect PolH and anti-PCNA. (B) Cell lysates were purified from RKO cells transfected with FLAG-tagged PolH, PolH-4KR, or PolH-Ub for 36 h and then subjected to immunoprecipitation with anti-PCNA or a control IgG followed by Western blotting with anti-FLAG to detect PolH and anti-PCNA. (C) *In vitro*-translated ^{35}S-labeled PolH or PolH-Ub was mixed with RKO cell lysates, which was then subject to immunoprecipitation with anti-PCNA or a control IgG. ^{35}S-labeled bound proteins were separated by SDS-PAGE for autoradiography, whereas PCNA was detected by Western blotting with anti-PCNA. (D) (Left panel) Western blots were prepared with lysates from RKO cells, which were immunodepleted with anti-PolH or control IgG immobilized on protein G-agarose beads and then detected with anti-PolH or antiactin. (Right panel) The experiment was performed as in panel C, except that PolH-depleted cell lysates were mixed with one of the three ^{35}S-labeled PolH proteins. (E) *In vitro*-translated ^{35}S-labeled PolH proteins (PolH, PolH-4KR, and PolH-Ub) were incubated with GST or GST-PCNA immobilized on glutathione-Sepharose beads for 4 h. ^{35}S-labeled bound proteins were eluted with SDS sample buffer and separated by SDS-PAGE for autoradiography.

monoubiquitinated in Pirh2 knockout (Pirh2-KO) MEF cells upon reconstitution of wild-type Pirh2 but not Pirh2-DN and Pirh2-ΔRING (Fig. 1L). Finally, mass spectrometry was performed to determine whether the slower-migrating band is monoubiquitinated PolH. We found that the slower-migrating band contained peptides derived from both PolH and ubiquitin (Fig. 2A and C), whereas the fast-migrating band contained peptides derived only from PolH (Fig. 2A and B). Together, these data suggest that PolH is a substrate of Pirh2 for monoubiquitination.

Identification of lysine residues in PolH for monoubiquitination by Pirh2. Three lysine residues, K682, K686, and K694, which are located within the nuclear localization sequence (NLS), and K709, which is located in the extreme C terminus in PolH, were found to be monoubiquitinated (2). To test whether monoubiquitination of these lysines were catalyzed by Pirh2, we generated 10 PolH mutants, which carry one, two, three, or four substitutions with arginine at K682, K686, K694, and K709 along with a FLAG tag (Fig. 3A). These PolH mutants were then expressed in RKO cells (Fig. 3B) and Pirh2-KO MEF cells (Fig. 3C), along with HA-tagged ubiquitin and Pirh2. We found that nine PolH mutants, which carry one to three arginine substitutions (K682R, K694R, K709R, K682.686R, K682.694R, K682.709R, K682.686.709R, K682.694.709R, and K682.686.694R), were still found to be monoubiquitinated (Fig. 3B and C). In contrast, little if any monoubiquitination was detected for the PolH mutant with a quadruple substitution of lysines with arginines (K682.686.694.709R, thereafter referred to as PolH-4KR) (Fig. 3B and C). These results suggest that Pirh2 monoubiquitinates PolH at one of the four lysine residues (K682, K686, K694, and K709).

Pirh2 suppresses PolH to interact with PCNA but not its sensitivity to proteasomal degradation via monoubiquitination of PolH. Recent studies showed that the switching from replicative polymerase δ (Pol δ) to TLS pol η is promoted by PCNA monoubiquitination (10, 17), but inhibited by PolH monoubiquitination (1, 2). These findings led us to test whether Pirh2 modulates the PCNA-PolH interaction through PolH monoubiquitination. To address this, FLAG-tagged PolH was expressed in RKO cells with or without Pirh2. We showed that a large fraction of PolH was monoubiquitinated in the presence

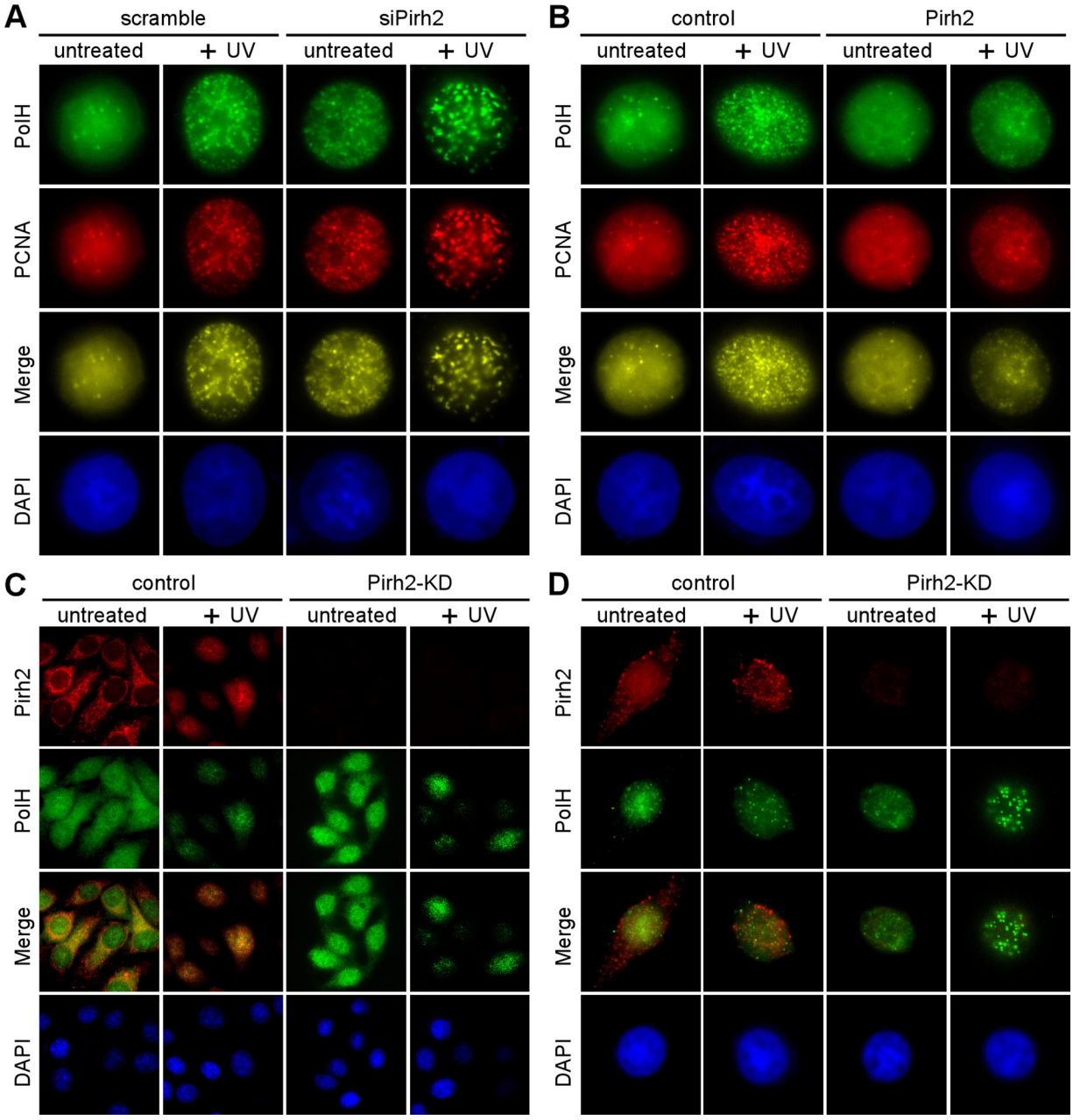

FIG. 5. Pirh2 regulates PolH-dependent translesion DNA synthesis. (A) XPV cells were cotransfected with GFP-PolH and FLAG-PCNA along with scramble or Pirh2 siRNA. After 72 h, cells were exposed to UV irradiation (15 J/m^2) and then incubated for 6 h. The PolH image was captured by GPF (green). The PCNA (red) image was obtained by anti-PCNA and Texas red-conjugated secondary antibody. Nuclei were visualized using 4′,6-diamidino-2-phenylindole (DAPI). (B) The experiment was performed as in panel A, except that Pirh2-expressing vector or a control vector was cotransfected. (C and D) RKO cells were uninduced (control) or induced to knock down Pirh2 (Pirh2-KD) for 72 h and then exposed to UV irradiation (15 J/m^2). Six hours after UV irradiation, PolH (green) was detected by anti-PolH and FITC-conjugated secondary antibody. Pirh2 (red) was detected by anti-Pirh2 and Texas red-conjugated secondary antibody. Images of multiple (C) and single (D) cells were obtained. (E) XPV cells were transfected with GFP-tagged PolH, PolH-Ub, PolH-4KR, and PolH-4KR-NLS along with scramble or Pirh2 siRNA. Representative GFP images were obtained 6 h after UV irradiation (15 J/m^2). (F) The experiment was performed as described in panel E, except that the GFP images of multiple cells were obtained. (G) The percentage of replication focus-positive cells (with more than 5 foci) was determined by counting at least 200 cells from three independent experiments.

of Pirh2 (Fig. 4A, lane 2), consistent with the above observation. We found that upon immunoprecipitation with anti-PCNA, PolH but not monoubiquitinated PolH was detected in PCNA immunocomplexes (Fig. 4A, lanes 5 and 6).

To further test this, we examined the interaction of PCNA with PolH-ubiquitin fusion protein (PolH-Ub), which contains the 76-aa ubiquitin fused at the C terminus of PolH polypeptide, or PolH-4KR, which cannot be monoubiquitinated, as shown above (Fig. 3). We showed that upon expression in RKO cells, wild-type PolH and PolH-4KR, but very little

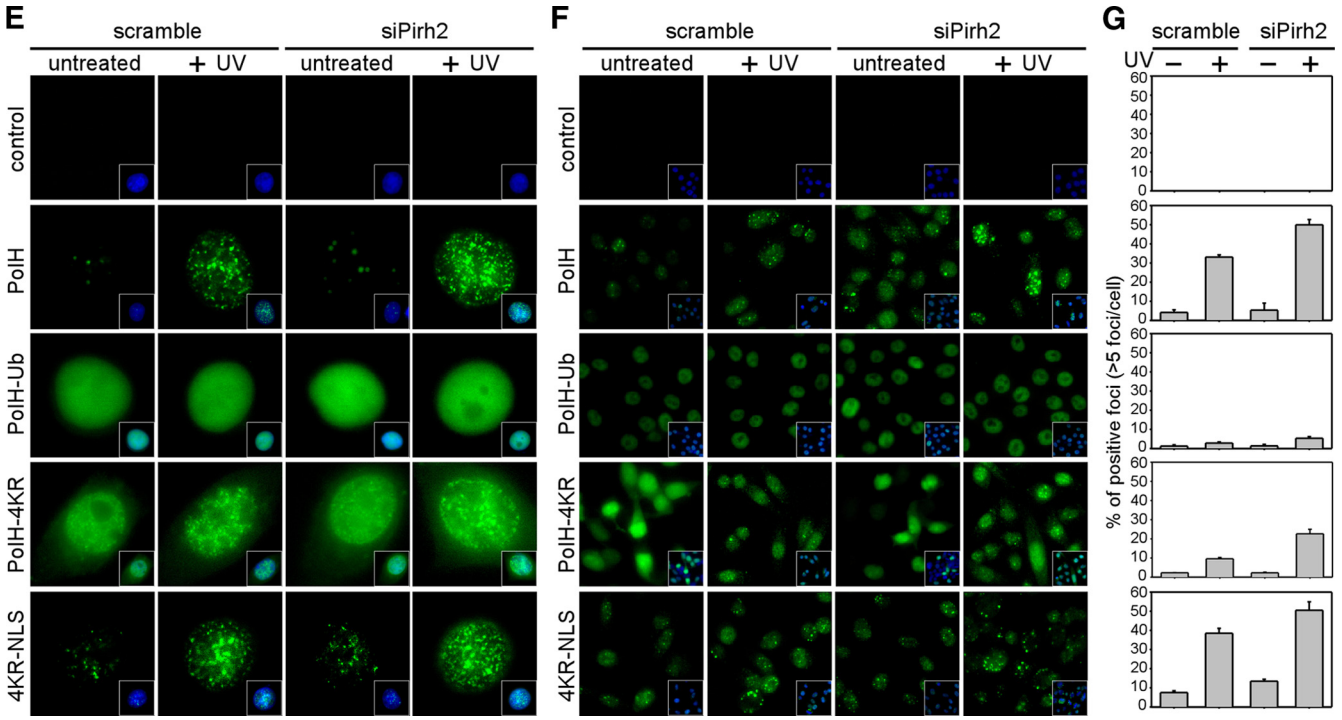

FIG. 5—*Continued.*

PolH-Ub, were detected in PCNA immunocomplexes (Fig. 4B, compare lanes 1 to 3 with lanes 7 to 9, respectively). Similarly, when *in vitro*-translated ^{35}S-labeled PolH or PolH-Ub mixed with PCNA-containing RKO cell extracts was subjected to immunoprecipitation with anti-PCNA, PolH, but very little PolH-Ub, was detected in PCNA immunocomplexes (Fig. 4C, compare lanes 1 and 2 with 5 and 6, respectively). In addition, when *in vitro*-translated ^{35}S-labeled PolH or mutant PolH (PolH-4KR and PolH-Ub) was mixed with PCNA-containing RKO cell extracts devoid of endogenous PolH through immunodepletion (Fig. 4D, left panel), endogenous PCNA was found to interact with PolH and PolH-4KR but very weakly with PolH-Ub upon immunoprecipitation with anti-PCNA (Fig. 4D, right panel, compare lanes 1 to 3 with lanes 7 to 9, respectively). Furthermore, the GST pulldown assay was performed with recombinant GST-tagged PCNA and *in vitro*-translated ^{35}S-labeled PolH. We found that wild-type PolH and PolH-4KR, but very little PolH-Ub, were found to directly interact with recombinant PCNA (Fig. 4E, compare lanes 1 to 3 with 7 to 9, respectively).

PolH is found to be degraded via the 20S proteasome, which is enhanced by Pirh2 (16). Thus, the *in vitro* protein degradation assay was performed and showed that like wild-type PolH, PolH-Ub and PolH-4KR were degraded by the 20S proteasome, which was inhibited by MG132 (see Fig. S1 in the supplemental material). This suggests that monoubiquitination does not decrease PolH sensitivity to proteasomal degradation.

Monoubiquitination decreases PolH-dependent translesion DNA synthesis. To examine whether monoubiquitination has an effect on PolH-dependent lesion bypass, UV irradiation was used to create DNA lesions. It is well established that upon UV irradiation, active DNA repair sites are loaded with various DNA repair proteins, including PolH and PCNA, which are termed "replication foci." To test this, XPV cells were transfected with GFP-tagged PolH and FLAG-tagged PCNA, along with siRNA against Pirh2. We found that upon UV irradiation, the numbers of PolH and PCNA replication foci were increased (Fig. 5A, two left panels) and were further increased by Pirh2 knockdown (Fig. 5A, two right panels). In contrast, the numbers of such replication foci were decreased by ectopic expression of Pirh2 (Fig. 5B). Similarly, we showed that upon UV irradiation, the replication foci of endogenous PolH in RKO cells accumulated (Fig. 5C and D, two left panels) and further increased in number by Pirh2 knockdown (Fig. 5C and D, two right panels). We also found that Pirh2 partially colocalized with PolH in response to UV irradiation (Fig. 5C and D). This implies an intimate link between Pirh2 and replication focus dynamics.

To further test this, we examined UV-induced focus formation of PolH in XPV cells expressing PolH, PolH-Ub, or PolH-4KR. We reasoned that if PolH-4KR is not subject to monoubiquitination, Pirh2 would have a limited effect on PolH-dependent lesion bypass. Alternatively, since PolH-Ub carries a ubiquitin, it would have limited PolH-mediated lesion bypass ability regardless of Pirh2. Indeed, we showed that the number of replication foci upon UV irradiation was increased markedly in PolH-producing XPV cells and weakly in PolH-4KR-producing XPV cells but not in PolH-Ub-producing XPV cells (Fig. 5E and F, two left panels). In addition, upon knockdown of Pirh2, the number of UV-induced PolH foci, but not PolH-4KR and PolH-Ub foci, was further increased (Fig. 5E and F, two right panels). Since three of the four lysine residues for monoubiquitination are located in the NLS, PolH-4KR may be deficient for being translocated to nucleus (2). To avoid potential aberrant effects of NLS mutations, an NLS sequence

from SV40 large T antigen was fused to the C terminus of PolH-4KR, and the resulting protein was designated PolH-4KR-NLS. Consistent with the previous report that PolH-4KR-NLS reacquires its ability to be translocated into nucleus (2), we found that upon UV irradiation, strong replication foci were detected in PolH-4KR-NLS-producing XPV cells (Fig. 5E and F, 4KR-NLS panel). Interestingly, while the number and size of replication foci in PolH-4KR-NLS-producing cells were slightly increased upon knockdown of Pirh2, the extent of the increase was much less than that of wild-type PolH (Fig. 5E and G, compare the PolH and PolH-4KR-NLS panels). The result is consistent with the idea that Pirh2-mediated PolH monoubiquitination regulates intracellular translocation and PolH-mediated lesion bypass.

To examine the biological significance of PolH monoubiquitination by Pirh2, we analyzed UV-induced cell death in MEF, RKO, H1299, and XPV cells. We found that upon knockout of Pirh2, UV-induced apoptosis was reduced from 25.41% to 11.83% in MEF cells (see Fig. S2A in the supplemental material). Similarly, upon knockdown of Pirh2 (in Fig. S2E in the supplemental material, compare lanes 1 and 2 for H1299 cells and compare lanes 3 and 5 for RKO cells), UV-induced apoptosis was reduced from 20.58% to 8.19% in H1299 cells (Fig. S2B) and from 16.67% to 8.47% in RKO cells (Fig. S2C). However, upon knockdown of PolH in RKO cells (in Fig. S2E, compare lanes 4 and 6), the effect of Pirh2 knockdown on UV-induced apoptosis was abrogated (21.38% versus 23.36%) (Fig. S2D). These results suggest that monoubiquitination of PolH by Pirh2 plays a role in bypassing UV-induced DNA damage and subsequently cell death. To further test this, we measured UV-induced cell death in XPV cells expressing PolH, PolH-Ub, PolH-4KR, or PolH-4KR-NLS. We showed that upon expression of PolH, the percentage of apoptosis in XPV cells was decreased from 32.42% for the control to 20.62% for PolH (Fig. 6A). PolH-Ub did not alleviate UV-induced apoptosis in XPV cells (Fig. 6A, 32.42% for control versus 33.11% for PolH-Ub), consistent with the lack of replication focus formation (Fig. 5E to G, PolH-Ub panel). Similarly, PolH-4KR had a weak effect (32.42% for control versus 26.17% for PolH-4KR), whereas PolH-4KR-NLS had a strong effect (32.42% for control versus 18.75% for PolH-4KR-NLS) on UV-induced apoptosis compared to wild-type PolH (Fig. 6A). This is also consistent with weak replication focus formation for PolH-4KR and strong replication focus formation for PolH-4KR-NLS (Fig. 5E to G, PolH-4KR, and PolH-4KR-NLS panels). However, while Pirh2 knockdown decreased the percentage of apoptosis in XPV cells expressing PolH or PolH-4KR-NLS, the extent of the reduction was much weaker in XPV cells expressing PolH-4KR-NLS (from 18.85% to 13.29%) than that in XPV cells expressing wild-type PolH (from 20.63% to 11.24%) (Fig. 6A). Finally, a clonogenic assay was performed with XPV (GM03617) cells to measure the effect of monoubiquitination on PolH-mediated lesion bypass along with treatment of caffeine as previously reported (19). Consistent with the extent of UV-induced replication arrest (Fig. 5E to G), the survival of XPV cells upon exposure to UV was rescued by PolH, PolH-4KR-NLS, and, to a lesser extent, by PolH-4KR compared to PolH-Ub (Fig. 6B). Together, these data suggest that PolH monoubiquitination modulates PolH-mediated translesion DNA synthesis and subsequently cell survival following UV irradiation.

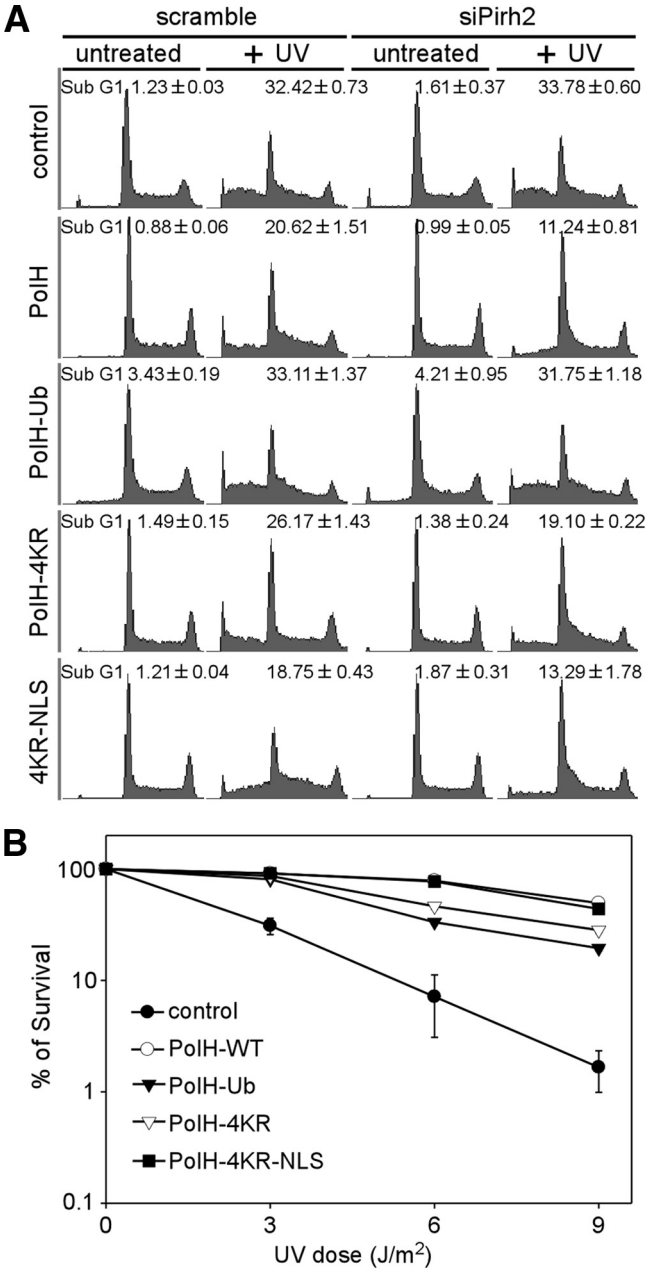

FIG. 6. Pirh2 regulates PolH-dependent resistance to UV irradiation. (A) XPV cells were transfected with GFP-tagged PolH, PolH-Ub, PolH-4KR, and PolH-4KR-NLS along with scramble or Pirh2 siRNA. After 72 h, cells were used for DNA histogram analysis 24 h post-UV irradiation (15 J/m^2). (B) The clonogenic assay was performed with XPV cells transfected with a control vector or a vector expressing wild-type PolH, PolH-Ub, PolH-4KR, or PolH-4KR-NLS. Cells were then incubated in DMEM containing 0.375 mM caffeine. Error bars represent the standard deviation (SD) from three independent experiments.

DISCUSSION

Previously, several reports have shown that PolH is regulated by phosphorylation (5) and covalent and noncovalent

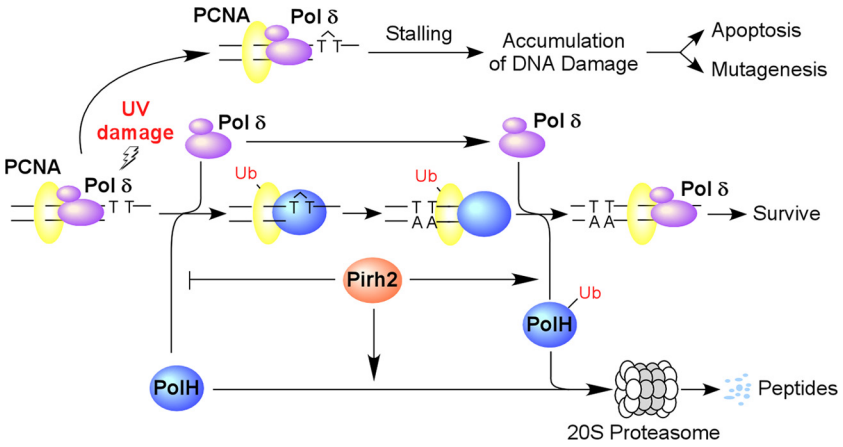

FIG. 7. Regulation of PolH expression and activity by Pirh2. Pirh2 promotes PolH monoubiquitination. Monoubiquitinated PolH protein is dissociated from the PCNA complex. Pirh2 recruits and targets PolH and monoubiquitinated PolH to the 20S proteasome for degradation. Pirh2 acts as a regulator to limit PolH-dependent translesion DNA synthesis once the UV-induced lesion is bypassed.

modifications with ubiquitin (1, 2, 26). However, the E3 ubiquitin ligase for PolH monubiquitination is still unknown. Here, we showed that Pirh2 E3 ubiquitin ligase promotes PolH monoubiquitination at multiple lysine residues *in vitro* and *in vivo*. We also showed that PolH monoubiquitination by Pirh2 inhibits its interaction with PCNA but has no effect on its degradation by 20S proteasome. Furthermore, we showed that the status of PolH monoubiquitination is associated with the ability of PolH to bypass UV-induced DNA lesions and consequently the viability of UV-damaged cells. Previously, we showed that Pirh2 physically interacts with and recruits PolH to 20S proteasome for degradation in a ubiquitin-independent manner (16). Moreover, we observed that Pirh2 knockdown leads to accumulation of PolH and subsequently enhances the survival of UV-irradiated cells (16). Based on these observations, we postulate that upon completion of TLS by PolH to bypass DNA lesions, including UV-induced DNA lesion, PolH is monoubiquitinated by Pirh2, which disengages PolH from inefficient and error-prone replication (Fig. 7). Monoubiquitination raises the possibility that Pirh2 carries out PolH degradation, but it is not yet clear how it might contribute to PolH degradation. It is also possible that deregulation of PolH by Pirh2 could hinder a proper level of TLS necessary for bypassing DNA lesions at both normal and stress conditions, leading to carcinogenesis. Indeed, Pirh2 has been found to be overexpressed in hepatocellular carcinoma (30), head and neck cancers (29), prostate cancer (22), and lung cancer (7). Therefore, a small compound that can specifically interfere with Pirh2 E3 activity and/or its interaction with PolH should be explored as a strategy to manage skin cancer and other diseases caused by UV irradiation.

We showed that Pirh2 monoubiquitinates PolH at one of the four lysine residues (K682, K686, K694, and K709). This finding raises an intriguing question: why is PolH, which can be monoubiquitinated at several sites, monoubiquitinated at only one site in a given molecule? One possibility is that due to the close proximity of the four lysine residues, ubiquitin conjugated to PolH at one lysine residue might inhibit further monoubiquitination by sterically hindering the access of Pirh2 to other lysine residues. Another possibility is that since PolH contains a UBZ domain, the ubiquitin conjugated to PolH at one lysine residue might be recognized by the UBZ domain, which would prevent PolH from being monoubiquitinated at other lysine residues.

In sum, upon completion of DNA lesions, Pirh2 appears to play a critical role in switching a low-fidelity translesion polymerase to a high-fidelity replicative polymerase via monoubiquitination. This leads us to hypothesize that monoubiquitination of PolH may trigger disengagement of PolH from PCNA and subsequently promotes its degradation. Thus, future studies are warranted to examine how Pirh2 mediates PolH degradation during DNA repair.

ACKNOWLEDGMENTS

We are grateful to Brett S. Phinney and Diana Tran for mass spectrometric analysis (UC Davis Proteomics Core Facility).

This work was supported by NIH grant CA123227 (X. Chen) and CIHR grant MOP-84459 (R. Hakem).

REFERENCES

1. **Bienko, M., et al.** 2005. Ubiquitin-binding domains in Y-family polymerases regulate translesion synthesis. Science **310:**1821–1824.
2. **Bienko, M., et al.** 2010. Regulation of translesion synthesis DNA polymerase eta by monoubiquitination. Mol. Cell **37:**396–407.
3. **Boutet, S. C., M. H. Disatnik, L. S. Chan, K. Iori, and T. A. Rando.** 2007. Regulation of Pax3 by proteasomal degradation of monoubiquitinated protein in skeletal muscle progenitors. Cell **130:**349–362.
4. **Chen, B. B., and R. K. Mallampalli.** 2009. Masking of a nuclear signal motif by monoubiquitination leads to mislocalization and degradation of the regulatory enzyme cytidylyltransferase. Mol. Cell. Biol. **29:**3062–3075.
5. **Chen, Y. W., et al.** 2008. Human DNA polymerase eta activity and translocation is regulated by phosphorylation. Proc. Natl. Acad. Sci. U. S. A. **105:**16578–16583.
6. **Cleaver, J. E., E. T. Lam, and I. Revet.** 2009. Disorders of nucleotide excision repair: the genetic and molecular basis of heterogeneity. Nat. Rev. Genet. **10:**756–768.
7. **Duan, W., et al.** 2004. Expression of Pirh2, a newly identified ubiquitin protein ligase, in lung cancer. J. Natl. Cancer Inst. **96:**1718–1721.
8. **Friedberg, E. C., R. Wagner, and M. Radman.** 2002. Specialized DNA polymerases, cellular survival, and the genesis of mutations. Science **296:** 1627–1630.
9. **Hicke, L., H. L. Schubert, and C. P. Hill.** 2005. Ubiquitin-binding domains. Nat. Rev. Mol. Cell Biol. **6:**610–621.
10. **Hoege, C., B. Pfander, G. L. Moldovan, G. Pyrowolakis, and S. Jentsch.** 2002. RAD6-dependent DNA repair is linked to modification of PCNA by ubiquitin and SUMO. Nature **419:**135–141.
11. **Hoeijmakers, J. H.** 2001. Genome maintenance mechanisms for preventing cancer. Nature **411:**366–374.

12. **Isasa, M., et al.** 2010. Monoubiquitination of RPN10 regulates substrate recruitment to the proteasome. Mol. Cell **38:**733–745.
13. **Johnson, E. S., P. C. Ma, I. M. Ota, and A. Varshavsky.** 1995. A proteolytic pathway that recognizes ubiquitin as a degradation signal. J. Biol. Chem. **270:**17442–17456.
14. **Johnson, R. E., C. M. Kondratick, S. Prakash, and L. Prakash.** 1999. hRAD30 mutations in the variant form of xeroderma pigmentosum. Science **285:**263–265.
15. **Jung, Y. S., et al.** 2008. Physical interactions and functional coupling between Daxx and sodium hydrogen exchanger 1 in ischemic cell death. J. Biol. Chem. **283:**1018–1025.
16. **Jung, Y. S., G. Liu, and X. Chen.** 2010. Pirh2 E3 ubiquitin ligase targets DNA polymerase eta for 20S proteasomal degradation. Mol. Cell. Biol. **30:**1041–1048.
17. **Kannouche, P. L., J. Wing, and A. R. Lehmann.** 2004. Interaction of human DNA polymerase eta with monoubiquitinated PCNA: a possible mechanism for the polymerase switch in response to DNA damage. Mol. Cell **14:**491–500.
18. **Kirkpatrick, D. S., et al.** 2006. Quantitative analysis of in vitro ubiquitinated cyclin B1 reveals complex chain topology. Nat. Cell Biol. **8:**700–710.
19. **Laposa, R. R., L. Feeney, and J. E. Cleaver.** 2003. Recapitulation of the cellular xeroderma pigmentosum-variant phenotypes using short interfering RNA for DNA polymerase H. Cancer Res. **63:**3909–3912.
20. **Leng, R. P., et al.** 2003. Pirh2, a p53-induced ubiquitin-protein ligase, promotes p53 degradation. Cell **112:**779–791.
21. **Liu, G., and X. Chen.** 2006. DNA polymerase eta, the product of the xeroderma pigmentosum variant gene and a target of p53, modulates the DNA damage checkpoint and p53 activation. Mol. Cell. Biol. **26:**1398–1413.
22. **Logan, I. R., et al.** 2006. Human PIRH2 enhances androgen receptor signaling through inhibition of histone deacetylase 1 and is overexpressed in prostate cancer. Mol. Cell. Biol. **26:**6502–6510.
23. **Logan, I. R., V. Sapountzi, L. Gaughan, D. E. Neal, and C. N. Robson.** 2004. Control of human PIRH2 protein stability: involvement of TIP60 and the proteosome. J. Biol. Chem. **279:**11696–11704.
24. **Masutani, C., et al.** 1999. The XPV (xeroderma pigmentosum variant) gene encodes human DNA polymerase eta. Nature **399:**700–704.
25. **Penengo, L., et al.** 2006. Crystal structure of the ubiquitin binding domains of rabex-5 reveals two modes of interaction with ubiquitin. Cell **124:**1183–1195.
26. **Plosky, B. S., et al.** 2006. Controlling the subcellular localization of DNA polymerases iota and eta via interactions with ubiquitin. EMBO J. **25:**2847–2855.
27. **Prakash, S., R. E. Johnson, and L. Prakash.** 2005. Eukaryotic translesion synthesis DNA polymerases: specificity of structure and function. Annu. Rev. Biochem. **74:**317–353.
28. **Sheng, Y., et al.** 2008. Molecular basis of Pirh2-mediated p53 ubiquitylation. Nat. Struct. Mol. Biol. **15:**1334–1342.
29. **Shimada, M., et al.** 2009. High expression of Pirh2, an E3 ligase for p27, is associated with low expression of p27 and poor prognosis in head and neck cancers. Cancer Sci. **100:**866–872.
30. **Wang, L., et al.** 2011. Interplay between MDM2, MDMX, Pirh2 and COP1: the negative regulators of p53. Mol. Biol. Rep. **38:**229–236.